Abundant non-inclusion α-synuclein pathology in Lewy body-negative LRRK2-mutant cases

Nanna Møller Jensen[1,2,*], Zagorka Vitic[1,2], Mia R. Antorini[1,2], Tobias Bruun Viftrup[1,2], Laura Parkkinen[3,4,#,*], Poul Henning Jensen[1,2,#,*]

[1]DANDRITE - Danish Research Institute of Translational Neuroscience, Aarhus C, Denmark.
[2]Department of Biomedicine, Aarhus University, Aarhus C, Denmark.
[3]Oxford Parkinson's Disease Centre, University of Oxford, Oxford, United Kingdom.
[4]Nuffield Department of Clinical Neurosciences, University of Oxford, Oxford, United Kingdom.
[#]These authors are shared last author.
*These authors are corresponding authors.

Abstract

Lewy body diseases are common neurodegenerative diseases, including Parkinson's disease (PD) and dementia with Lewy bodies, which lead to both motor and non-motor symptoms. They are neuropathologically characterized by loss of neuromelanized neurons in the substantia nigra pars compacta and α-synuclein-immunopositive inclusions (Lewy bodies) in several types of neurons in the brain. A fraction of monogenic PD cases, however, represent a conundrum, as they can present with clinical Lewy body disease but do not have Lewy bodies upon neuropathological examination. For LRRK2, the presence or absence of Lewy bodies is not related to any specific mutation in the gene and different clinical presentation and neuropathology can be present even in the same family.

Here, we present the first evidence of widespread α-synuclein accumulation detected with proximity ligation assay (PLA) using the MJFR14-6-4-2 antibody in six Lewy body-negative LRRK2 cases and compare the levels with five patients with neuropathologically-verified Lewy body disease cases and six healthy controls. We show that non-inclusion, aggregated α-synuclein PLA signal is dominant in the LRRK2 cases, while Lewy-like PLA signal is predominant in late-stage Lewy body disease. Furthermore, LRRK2 cases displayed prominent PLA signal in pontocerebellar tracts and inferior olivary nuclei in the brainstem, which was not seen in idiopathic PD cases. These results suggest that Lewy-body negative LRRK2-related PD is not associated with a lack of α-synuclein aggregation in neurons but rather a deficiency in the formation of inclusions.

Keywords: α-synuclein, Lewy body disease, LRRK2, neurodegeneration, non-inclusion pathology, proximity ligation assay

Introduction

Lewy body diseases (LBDs), a collective term encompassing Parkinson's disease (PD), PD with dementia (PDD), and dementia with Lewy bodies (DLB), are common and debilitating neurodegenerative diseases [32, 45]. They feature varying degrees of motor symptoms (resting tremor, rigidity, and bradykinesia) as well as non-motor dysfunctions, such as hyposmia, sleep disturbances, gut dysfunction, depression, and dementia [32, 56]. Neuropathologically, PD is defined by neuronal loss particularly in the substantia nigra pars compacta (SNpc) as well as characteristic proteinaceous inclusions in the neurons of multiple brain regions [14]. The inclusion pathology, encompassing Lewy bodies (LBs) in

the soma and Lewy neurites (LNs) in neuronal processes, present in stereotypical patterns used to stage disease severity [3, 9]. Aggregated forms of the neuronal protein α-synuclein, phosphorylated on serine-129, are found in these inclusions in both PD and DLB [14, 41]. Though most PD cases are idiopathic, mutations in a number of genes can cause autosomal dominant and recessive forms of monogenic PD, which constitute approx. 10-15% of cases [5, 13, 32, 47, 48]. Of these, mutations in the leucine rich repeat kinase (LRRK2) have been particularly puzzling, as some LRRK2 patients are clinically diagnosed with PD but do not contain LBs upon autopsy [33, 48, 72]. This has led to discussion whether these LB-negative LRRK2-PD cases also represent a synucleinopathy or a completely different aetiology not associated with α-synuclein aggregation [10, 33, 42, 57, 63].

In this study, we used an α-synuclein aggregate-specific proximity ligation assay (PLA), which detects non-inclusion α-synuclein aggregates preceding regular Lewy pathology, to study six cases of LB-negative LRRK2 cases. Based on dual antibody recognition followed by a rolling circle signal amplification, α-synuclein PLA has become a predominant strategy to detect small, oligomeric α-synuclein aggregates, which are undetected by immunohistochemistry [31, 51, 60, 61]. In the present study, we used the conformation-specific MJFR14-6-4-2 antibody in a PLA application that detects α-synuclein aggregate pathology whether organized into inclusions (i.e., LBs and LNs) or not (i.e., oligomeric) [31]. The PLA staining patterns from LB-negative LRRK2 cases were compared with five idiopathic LBD (Braak stage 6) and six healthy controls. We demonstrate that these LRRK2 cases consistently display α-synuclein PLA-positive pathology and typically at higher levels than regular LBD cases, while most controls only present with very little PLA signal. These results indicate that α-synuclein aggregation is also a characteristic of LB-negative LRRK2 cases. As such, LB-negative LRRK2 cases may be associated with an inability to form LBs and LNs, rather than a lack of α-synuclein aggregate pathology.

Materials and methods

Human tissue

Brains from LB-negative LRRK2 cases (n = 6), idiopathic LBD (n = 5), and healthy control (n = 6) were obtained from Parkinson's UK Brain Bank (PUKBB), Imperial College London, and Oxford Brain Bank (OBB), Nuffield Department of Clinical Neurosciences in University of Oxford, in accordance with approved protocols by the Wales Research Ethics Committee (23/WA/0273) and the Ethics Committee of the University of Oxford (ref 23/SC/0241). All participants had given prior written informed consent for the brain donation. Both brain banks comply with the requirements of the Human Tissue Act 2004 and the Codes of Practice set by the Human Tissue Authority (HTA licence numbers 12275 for PUKBB and 12217 for OBB). Formalin-fixed paraffin embedded (FFPE) tissue sections of 5 µm thickness from the medulla, pons, midbrain, posterior hippocampus, and amygdala were included in the study. Cases included and their clinical, pathological, and genetic data are summarized in Table 1.

Proximity ligation assay

Conformation-specific α-synuclein antibody MJFR14-6-4-2 (MJF-14; Abcam, #ab214033, 1 mg/mL) was conjugated to complementary NaveniLink proximity probes (Navinci, #NL.050) according to manufacturer's instructions. Briefly, 10 µL of Modifier was added to 100 µL antibody, before mixing with the lyophilized oligonucleotides (Navenibody 1 or Navenibody 2) and incubation overnight at room

temperature (RT). 10 µL of Quencher N was then added and incubated for 15 minutes at RT, whereafter conjugated antibodies were stored at 4°C.

The PLA staining was conducted using NaveniBright HRP kits using DAB as the chromogen (Navinci, #NB.MR.HRP.100) and counterstained with a haematoxylin-based nuclear dye. FFPE sections were deparaffinized and rehydrated in decreasing alcohol series, before antigen retrieval of microwaving for 2x 5 min. in sodium citrate (pH 6, DAKO, #S1699). Endogenous peroxidase activity was quenched in 0.3% hydrogen peroxide in PBS, after which samples were blocked in Navinci blocking buffer with supplement 1 for 1 hour at 37°C. PLA-conjugated MJF-14 was diluted 1:10,000 in antibody diluent with supplement 2 and incubated with the samples overnight at 4°C. After washing off unbound antibody, samples were incubated in freshly prepared Reaction 1 (1x Buffer 1 diluted in nuclease-free water and supplemented with Enzyme 1) for 30 min at 37°C. Subsequently, Reaction 2 was similarly prepared (1x Buffer 2 diluted in nuclease-free water and supplemented with Enzyme 2) and applied for 60 min at 37°C. Sections were then incubated in HRP detection solution for 30 min at RT, before signal development for 5 min at RT. Finally, sections were briefly counterstained in Navinci Nuclear stain and staining developed in tap water, before a quick dehydration in 100% isopropanol and mounting with VectaMount Express Mounting Medium (VectorLabs, #H-5700).

Imaging and analysis

Tissue sections were imaged at X20 magnification on an Olympus VS120 slide scanner and stored in the vsi file format. Digitalized images were opened in QuPath [2], stain vectors estimated using the auto function, and the entire tissue regions were outlined by thresholding on averaged channel values. Specific regions of interest were annotated according to The Brain Atlas and specific articles pertaining individual subregions [1, 25, 58, 68, 71].

5 total slide scans were selected to optimize parameters for detection of signals for quantitative image analysis. These cases (LBD 1 medulla, LBD 1 pons, LRRK2 6 midbrain, LRRK2 1 posterior hippocampus, and LRRK2 4 amygdala) encompassed different composition and densities of the various signals found across the cohort. Signals were divided into particulate PLA signal (not associated with inclusions) and Lewy-like PLA signal (signal found in structures resembling LBs and LNs) and quantified as area coverage (%) to allow a direct comparison between the two measures

For all analyses, groups were compared using a non-parametric Kruskal-Wallis followed by Dunn's multiple comparison test, as data did not pass normality tests. P-values under 0.05 were considered significant (* $p<0.05$, ** $p<0.01$, *** $p<0.001$), though values close to significance were also indicated, as the small group sizes and non-parametric tests limit the chance of reaching statistical significance. Graphs and statistics were performed in GraphPad Prism 10, and figures created with Adobe Illustrator and BioRender (publication license: Jensen, N. (2025) https://BioRender.com/l05s274).

Results

The study included six LRRK2 cases, all of which were LB-negative on standard neuropathological assessments. Three of the cases had a clinical diagnosis of PD, one a diagnosis of progressive supranuclear palsy (PSP, neuropathologically confirmed), and two cases had no clinical diagnoses of

neurodegenerative disease. These were compared with five idiopathic LBD cases, all of which were Braak stage 6, and six healthy controls, as based on standard clinicopathological assessments.

Case ID	Clinical diagnosis	Sex	Age at death (years)	Braak PD stage	LRRK2 mutation(s)
LRRK2 1	PD	M	92	LB-negative	M1646T
LRRK2 2	–	F	94	LB-negative	N2081D
LRRK2 3	–	F	87	LB-negative	M1646T
LRRK2 4	PSP	F	61	LB-negative	N2081D
LRRK2 5	PD	M	84	LB-negative	N2081D, M1646T, P1542S
LRRK2 6	PD	F	79	LB-negative	G2019S, N2081D
LBD 1	PD	M	78	6	–
LBD 2	DLB	M	85	6	–
LBD 3	PD	M	80	6	–
LBD 4	DLB	F	79	6	–
LBD 5	PD	F	81	6	–
Control 1	Healthy control	F	88	0	–
Control 2	Healthy control	M	82	0	–
Control 3	Healthy control	M	78	0	–
Control 4	Healthy control	M	70	0	–
Control 5	Healthy control	F	89	0	–
Control 6	Healthy control	F	89	0	–

Table 1 Demographics, clinical characteristics, and LRRK2 mutations in the cohort
DLB = dementia with Lewy bodies, LBD = Lewy body disease (PD/PDD/DLB), PD = Parkinson's disease, PSP = progressive supranuclear palsy.

From each case, FFPE sections from five brain regions were stained with an α-synuclein aggregate PLA using the MJF-14 antibody (Fig. 1a, Suppl. Fig. 1). The PLA staining produced two distinct patterns of signal, 1) punctate PLA particles that appeared to locate to the neuropil and were not associated with neuronal inclusions, called "particulate PLA" (Fig. 1b, top) and 2) a Lewy-like PLA signal strongly resembling the LBs and LNs stained by regular IHC (Fig. 1b, bottom). The two patterns of signal were distinguished based on their colour and intensity, as the Lewy-like PLA signal (formed by coalescing of highly abundant PLA particles) appeared intensely almost reddish black.

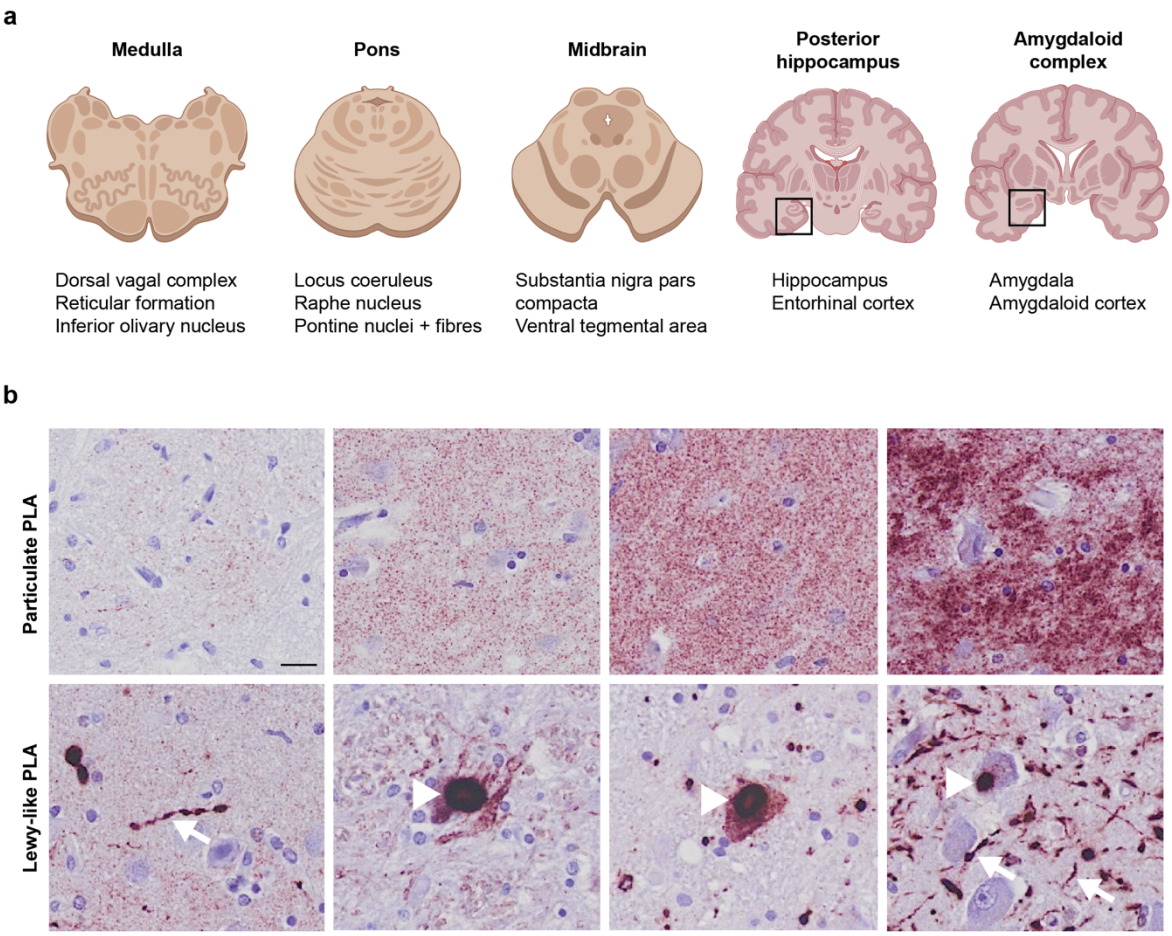

Fig. 1 Regions of interest and PLA terminology

a) Five brain regions (medulla, pons, midbrain, posterior hippocampus, and amygdala) were included for each case to allow comparative quantitative analyses of PLA signals. See Suppl. Fig. 1 for delineation of the listed subregions in three of the cases included in this study. **b**) The PLA staining yielded two distinct patterns of signal: the particulate PLA not associated with inclusions (top panels) with increasing signal density from left to right and a Lewy-like PLA staining (bottom panel) with strong morphological similarity to LBs and LNs as stained by standard IHC. Presumed LBs are indicated by arrowheads, while examples of putative LNs are highlighted with arrows. Scale bar = 20 µm (applies to all images). Particulate and Lewy-like PLA were analysed separately in all sections and reported as area covered (%). Brain region graphic in **a** was created in BioRender. Jensen, N. (2025) https://BioRender.com/l05s274.

LRRK2 cases show abundant particulate PLA, while both particulate and Lewy-like PLA is found in LBD cases

As expected from the case inclusion criteria, Lewy-like PLA signal was almost exclusively present in the Braak stage 6 LBD cases, where it was found in all regions analysed (Fig. 2a, c). The Lewy-like PLA encompassed both LBs and LNs, the latter of which were abundant in e.g. the CA2 of the hippocampus (Fig. 2a). Only very little Lewy-like PLA signal was detected in either LB-negative LRRK2 cases or healthy controls (Fig. 2c). In contrast, particulate PLA signal was predominant in the LRRK2 cases, of which all six contained signal, while some particulate PLA signal was found in LBD cases and a two of controls as well (Fig. 2a-b). Particulate PLA was especially prominent in the posterior hippocampus and amygdala sections of the LRRK2 cases, where an average of 8-10% of the total areas were covered with

particulate PLA signal (Fig. 2b). On average, the LB-negative LRRK2 cases contained 2.5-10 times more particulate PLA signal than the LBD cases when analysing the entire tissue sections, though group differences did not reach statistical significance (Fig. 2b). Furthermore, even in the LBD cases, the particulate PLA signal was much more abundant than the Lewy-like PLA signal, in line with previously published studies using α-synuclein PLA in LBD cases [31, 60, 61]. Of note, the ratio between particulate and Lewy-like PLA increased with more rostral sections, with an average area coverage from 41-fold higher in medulla to more than 100-fold higher in posterior hippocampus and amygdala sections (Fig. 2b-c, Suppl. Table 1). Based on the limited cohort in this study, we could not conclude whether this difference in signal ratio was related to region-specific propensities for forming LBs (brainstem versus limbic/cortical), a rostral progression of disease, or other yet unknown causes.

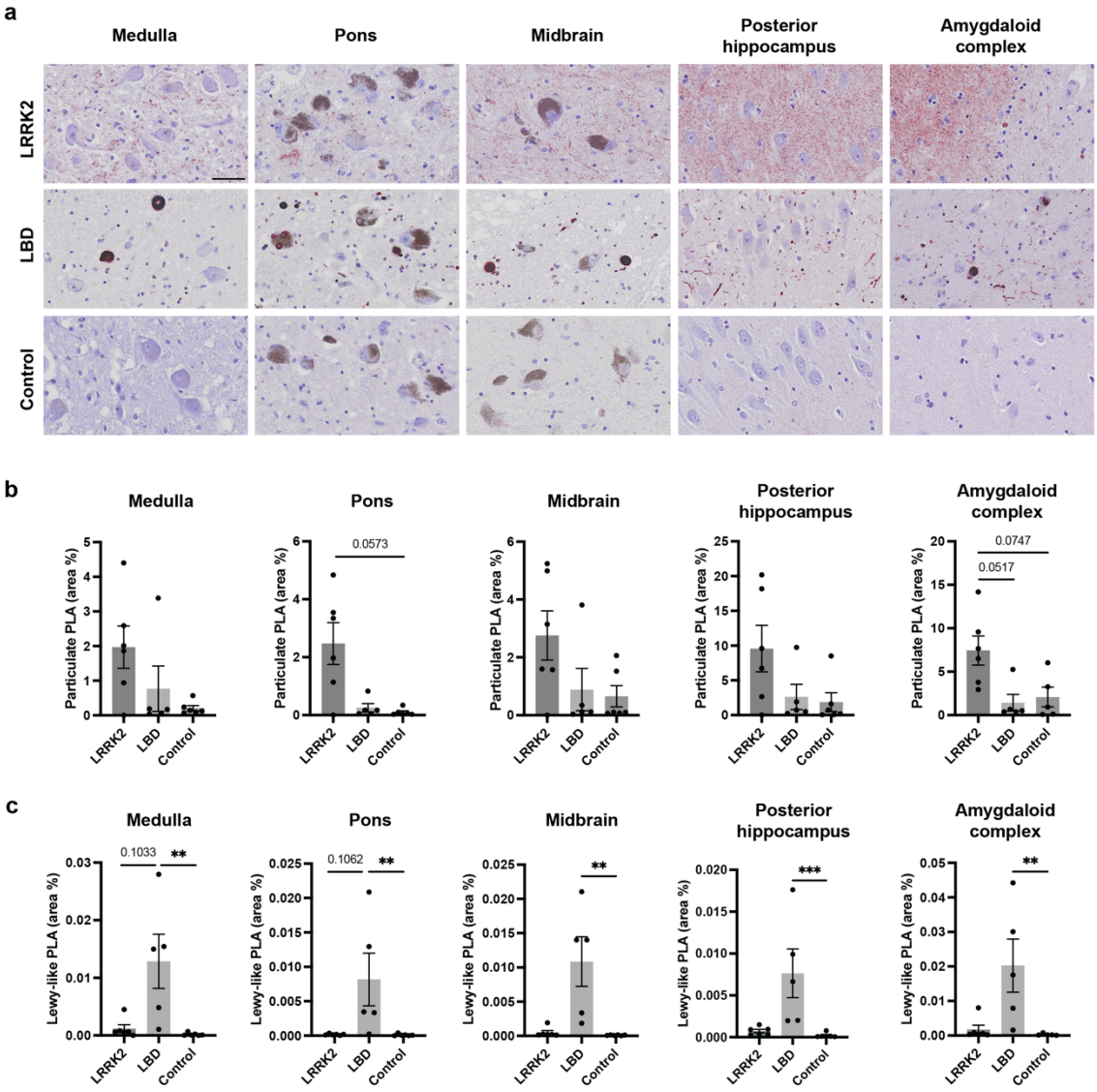

Fig. 2 Particulate PLA, Lewy-like PLA, and LB densities in LRRK2 LB-negative cases, regular LBD, and non-neurodegenerative controls

a) Overview of PLA staining appearance in medulla (around DMV), pons (around LC), midbrain (around SNpc), posterior hippocampus (around CA2), and amygdaloid complex (in the amygdala). Scale bar = 50 µm (applies to all images). **b-c**) Quantitative analysis performed in the entire tissue sections showing particulate PLA area coverage (%, **b**) and Lewy-like PLA area coverage (%, **c**) for the three groups. All graphs show

mean ± SEM with data points for individual cases. Analysed with Kruskal-Wallis one-way ANOVA followed by Dunn's multiple comparison test. * $p<0.05$, ** $p<0.01$, *** $p<0.001$. CA2 = cornu ammonis 2 of the hippocampus, DMV = dorsal motor nucleus of the vagus, LC = locus coeruleus, SNpc (substantia nigra pars compacta).

LRRK2 cases display varying amounts of particulate PLA signal in nuclei and regions typically affected in PD but also in unusual regions

A closer examination of the distribution of particulate PLA signal in the LRRK2 cases showed signal in most classical PD regions such as the dorsal motor nucleus of the vagus (DMV), LC, SNpc and ventral tegmental area (VTA) (Fig. 3, see also Suppl. Fig. 1 for representative overviews and delineation of regions). The idiopathic LBD cases generally showed similar levels of particulate PLA in these nuclei and regions, in addition to the prominent LBs (Fig. 3, Suppl. Fig. 2).

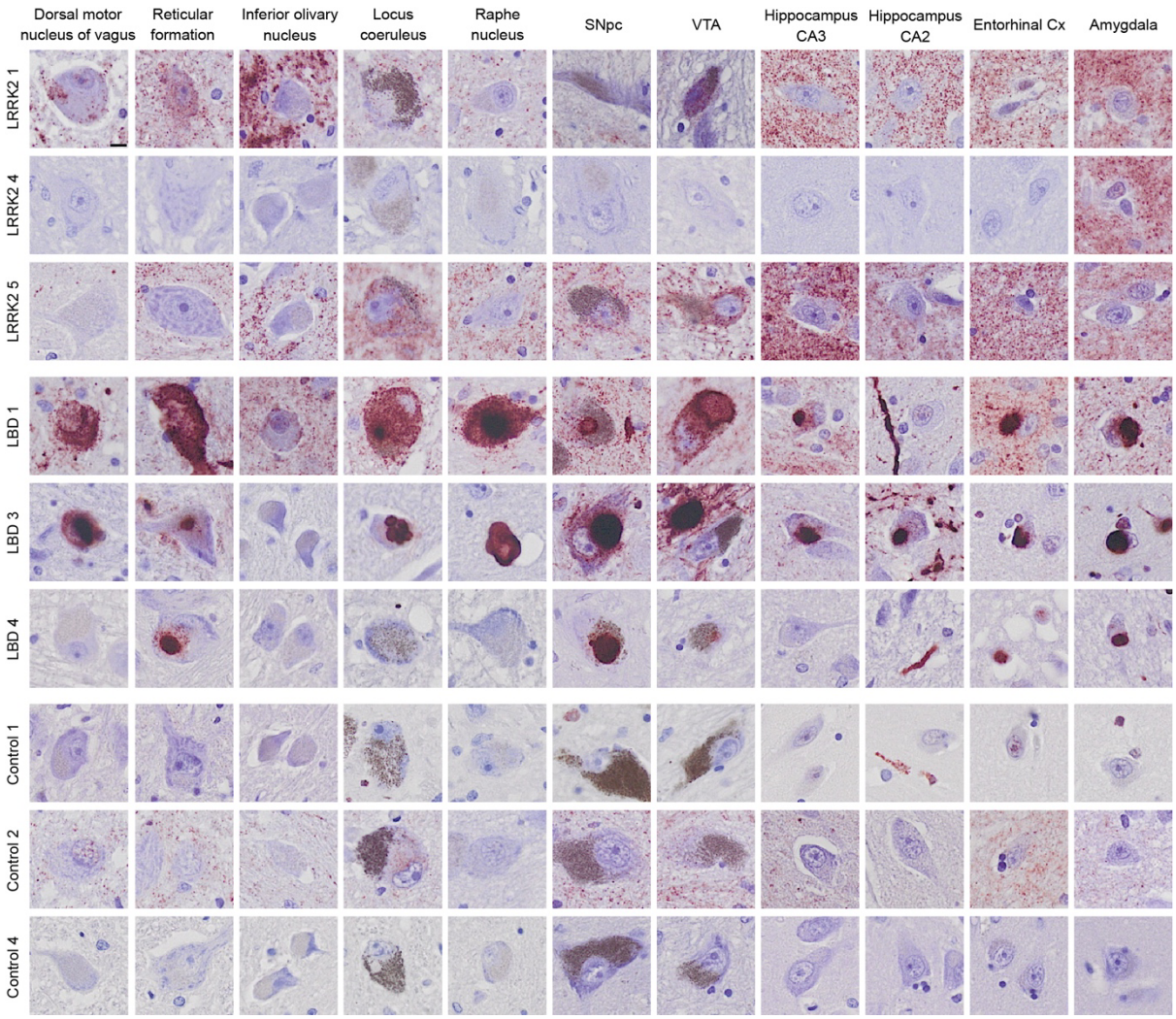

Fig. 3 PLA signal in specific brain regions from selected cases

Specific brain regions were identified from the medulla (dorsal vagal complex, reticular formation, and inferior olivary nucleus), pons (locus coeruleus and raphe nucleus), midbrain (substantia nigra pars compacta, SNpc, and ventral tegmental area, VTA), posterior hippocampus (CA3, CA2, and entorhinal cortex)

and amygdala. Three cases were displayed from each group, encompassing most of the variation in signal densities in each group. Scale bar = 10 µm (applies to all images). Note that LRRK2 4 was almost entirely depigmented and had substantial neuronal loss in several regions, incl. SNpc. See also semi-quantitative overview particulate versus Lewy-like PLA in all cases in Fig. 6.

However, the particulate PLA in LRRK2 cases was especially prominent in regions not typically affected in PD, such as the inferior olivary nucleus (ION) (Fig. 4) and the basilar pons (Fig. 5). In five of the six LRRK2 cases, the ION contained noteworthy particulate PLA signal, while only one of five LBD cases displayed signal in this region (Fig. 4). Of note, where the particulate PLA in the LRRK2 cases was confined to the neuropil, sparing the cell bodies of ION neurons, LBD 1 showed particulate PLA signal in both the neuropil and the ION neurons (Fig. 4b, arrows). In the basilar pons, the transverse, pontocerebellar fibres were highly positive for particulate PLA in the same five of six LRRK2 cases, along with varying positivity in the pontine nuclei (Fig. 5a-b). The longitudinal fibres, which encompass the ascending and descending corticospinal and corticonuclear fibres, only contained negligible levels of particulate PLA signal (Fig. 5a-b). In the LBD cases, in comparison, the pontine nuclei and transverse, pontocerebellar fibres only contained low levels of signal, whether particulate or Lewy-like PLA (Fig. 5a, c). As for the LRRK2 cases, the longitudinal fibres were generally negative for any PLA signal in the LBD cases as well, except for LBD 5 in which some Lewy-like PLA signal was found (Fig. 5c, arrows).

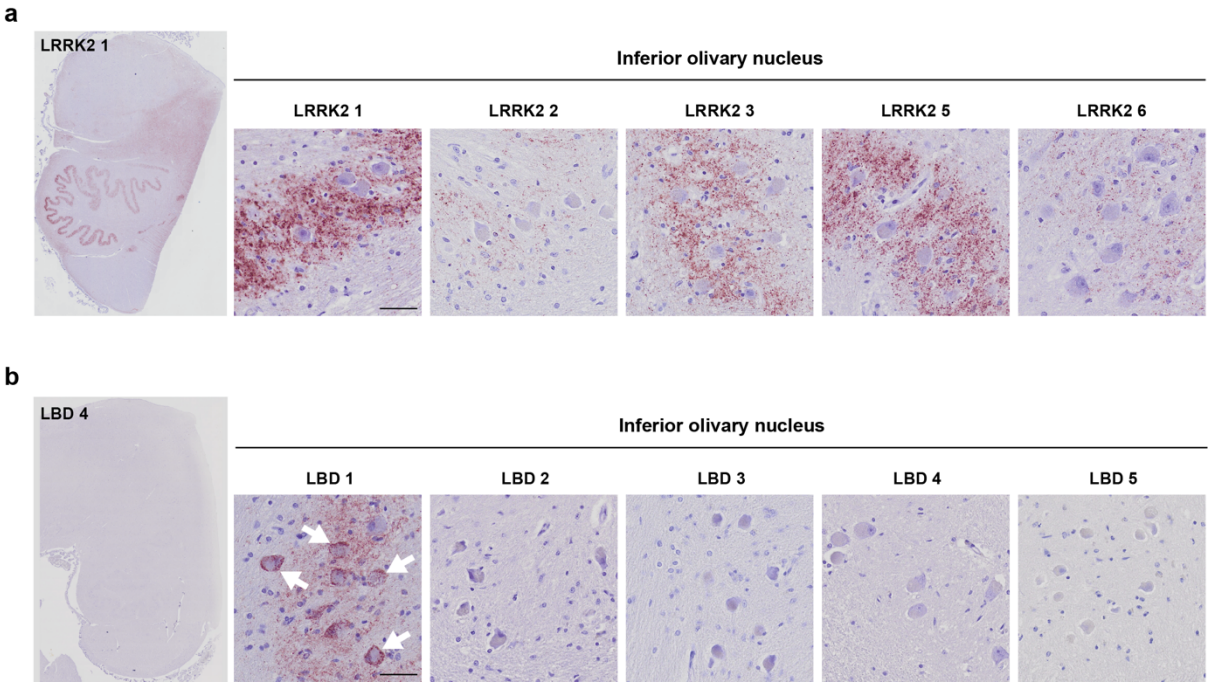

Fig. 4 Prominent PLA signal in the inferior olivary nucleus of LRRK2 cases

a) LRRK2 cases displayed particulate PLA signal in the inferior olivary nucleus, with signal predominantly present in the neuropil surrounding the neuronal cell bodies. Note that LRRK2 4, which contained no PLA signal in the medulla, was left out of the figure. **b**) Only LBD 1 of the LBD cases displayed PLA signal in the inferior olivary nucleus. Note that in this case, signal is not confined to the neuropil but also found in the neuronal cell bodies. Scale bars = 50 µm. See also semi-quantitative overview particulate versus Lewy-like PLA in all cases in Fig. 6.

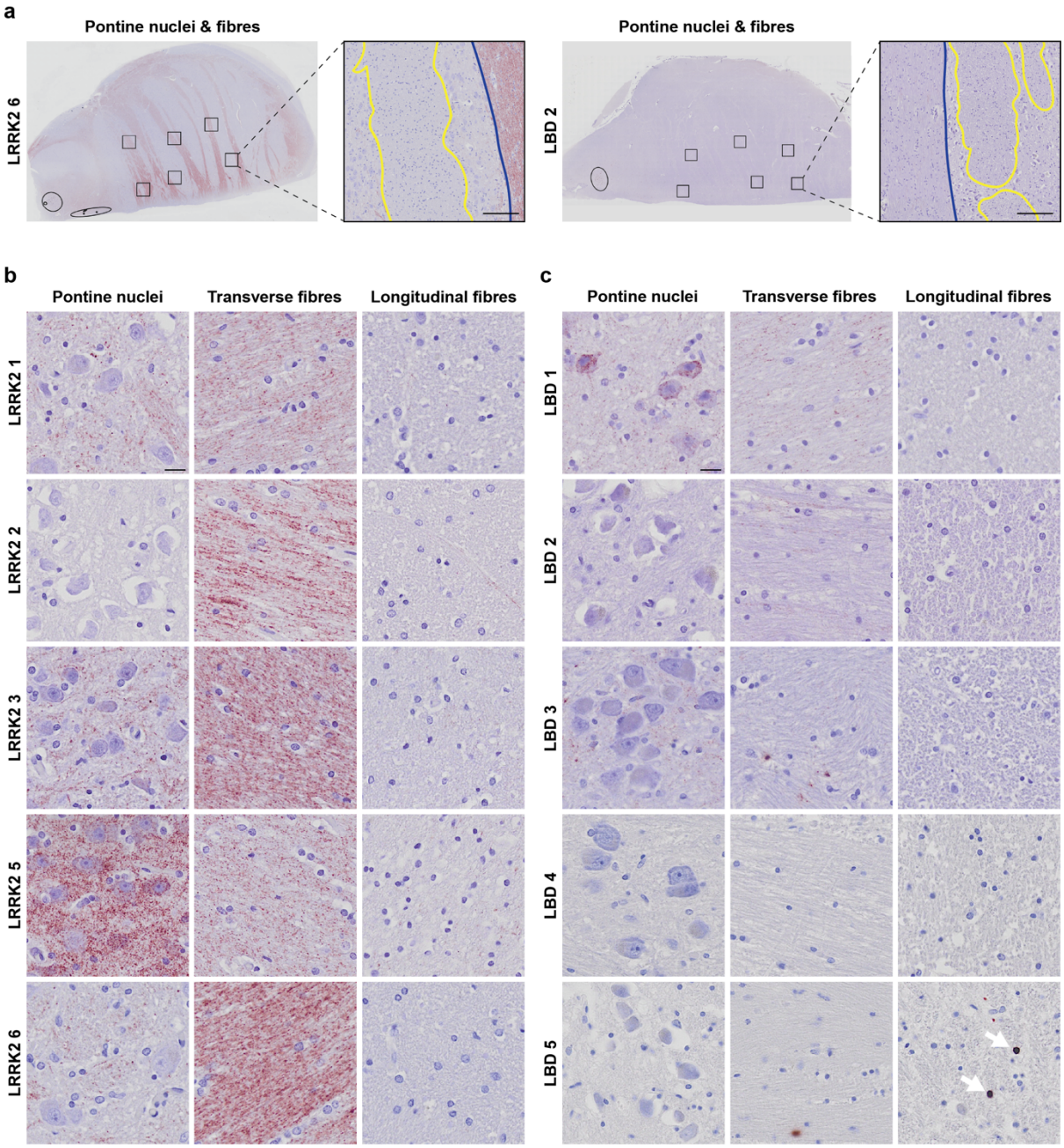

Fig. 5 PLA in pontine nuclei, transverse and longitudinal fibres of the basilar pons

a) Particulate and Lewy-like PLA signal was assessed in six ROIs in the basilar pons of all cases as indicated in the overviews from one LRRK2 case (left) and one LBD case (right). Magnified panels show transverse fibres (outlined in blue) and longitudinal fibres (outlined in yellow), while in-between areas correspond to pontine nuclei. Scale bars = 200 µm. **b**) LRRK2 cases displayed dense particulate PLA signal in the transverse (pontocerebellar) fibres and to some degree in the pontine nuclei. Note that LRRK2 4, which was negative in the pons, was left out of the figure. Scale bar = 20 µm (applies to all images). **c**) LBD cases displayed much less signal in pontine nuclei and transverse fibres than the LRRK2 cases. One case (LBD 5) presented with some Lewy-like PLA signal in the longitudinal fibre bundles (arrows). Scale bar = 20 µm (applies to all images). See also semi-quantitative overview particulate versus Lewy-like PLA in all cases in Fig. 6.

In addition to the prominent brainstem pathology, five out of six LRRK2 cases displayed high levels of particulate PLA in hippocampus and entorhinal cortex, and all cases in amygdala-associated cortex (Fig. 3, Suppl. Fig. 1, Suppl. Fig. 2). In the hippocampus, particulate PLA signal was found in all hippocampal subregions (dentate gyrus as well as CA1-3), though the specific distribution varied between cases. In entorhinal and amygdala-associated cortex, particulate PLA signal was present in both the superficial (layers 1-3) and deep cortical layers (layer 5-6), without any obvious difference in signal density. This was observed for both the LRRK2 cases and the LBD cases, though LBs were selectively accumulated in the deep cortical layers, in line with previous reports from us and others [8, 26, 31].

Healthy control cases generally displayed low particulate PLA signal, though two cases showed some abundance around specific neuronal populations in the DMV, SNpc, and amygdala (see Controls 2 and 6, Fig. 3 and semi-quantitative overview in Fig. 6).

As already seen in the quantifications in Fig. 2 and Suppl. Fig. 2, there was quite a lot of variation in signal density (both particulate PLA and Lewy-like PLA) within the LRRK2 and LBD case groups, respectively. One of the LRRK2 cases (LRRK2 4) stood out amongst the cases with profound particulate PLA in the amygdala alone, while all other regions were unaffected (Fig. 3, Fig. 6a). All of the other LRRK2 cases had significant particulate PLA in all brain sections examined, although the densities and regional distributions differed. Curiously, the LRRK2-mutation present in LRRK2 4 (N2081D) was also present in LRRK2 2 (and in LRRK2 5 and 6 along with additional mutations), indicating that the unique staining pattern in LRRK2 4 cannot be solely ascribed to the N2081D LRRK2-mutation (Table 1). Alternatively, either the clinical diagnosis of progressive supranuclear palsy (PSP), which was the only tauopathy diagnosis in the cohort, the relatively young age at death compared to the other LRRK2 cases, or other factors may affect the presence of particulate PLA.

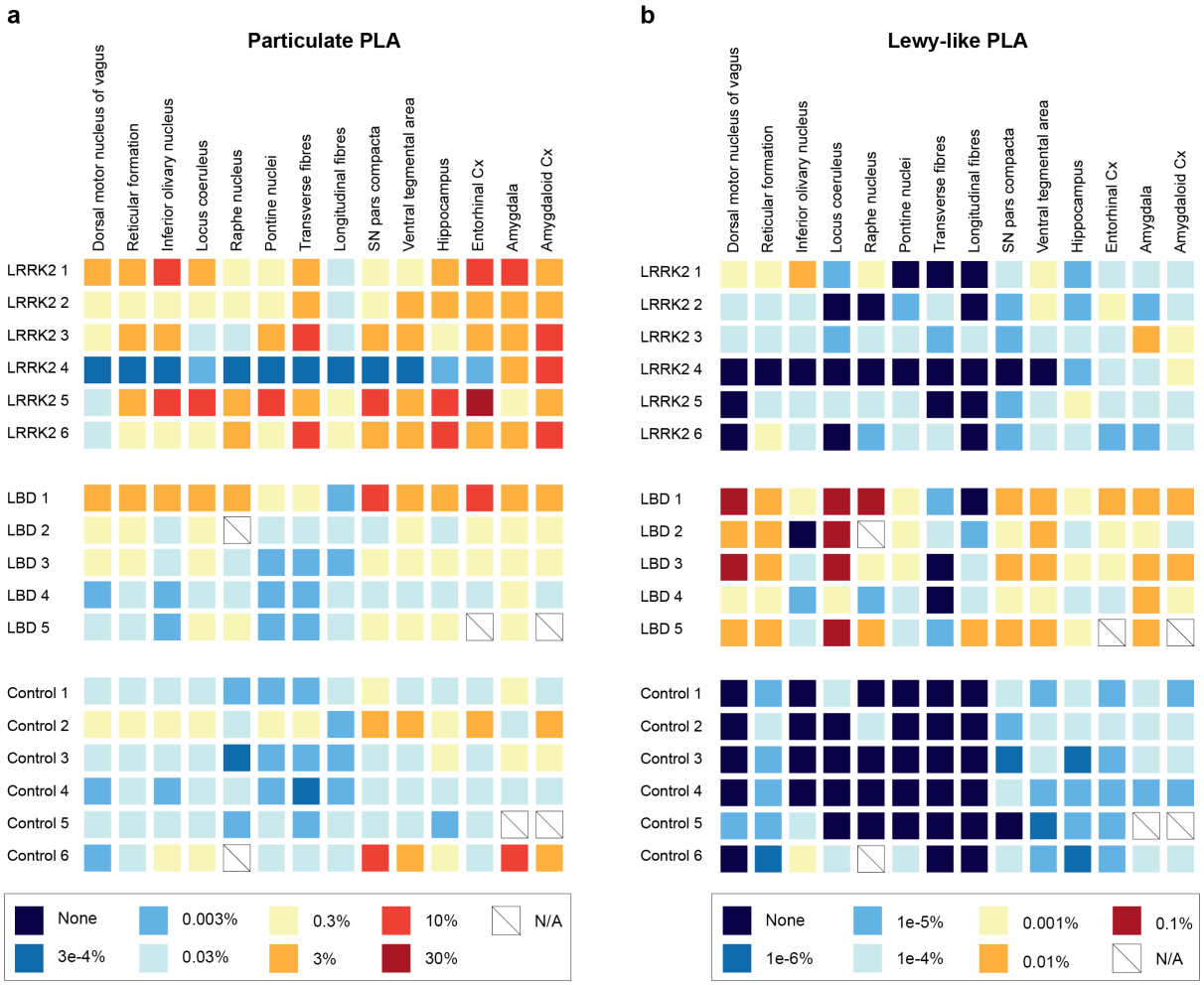

Fig. 6 Graphical summary of particulate and Lewy-like PLA across all cases and nuclei/regions examined

Based on the quantifications of area coverage, semi-quantitative scales were made for particulate PLA (**a**) and Lewy-like PLA (**b**). Note that the same colour in **a** and **b** denotes a 300-fold difference in area %. LBD cases stand out with a high density of Lewy-like PLA across the regions examined, while LRRK2 cases display the highest particulate PLA density. N/A, not available.

Neuronal loss may explain some of the variation in PLA signal density between cases

One of the factors likely affecting the signal densities observed in the LRRK2 and LBD cases is the neuronal loss in multiple brain regions, which is well-characterized for PD [14, 17, 19, 43]. In a few cases, including LRRK2 4 and LBD 4, brainstem nuclei such as the LC and SNpc were almost entirely depigmented and only few neurons were left. Though we did not specifically assess the cell loss, significant loss of cells in these nuclei may have resulted in a lower signal density, both for the particulate and the Lewy-like PLA. Indeed, LBD 4 for example, presented with lower signal density in the LC than the other LBD cases and also contained substantially fewer neurons in this region upon closer examination (Fig. 6 and Fig. 7). As a corroborating feature, supporting neuronal cell loss, we also observed extra-neuronal neuromelanin in several of the cases [14] (Fig. 7, arrowheads).

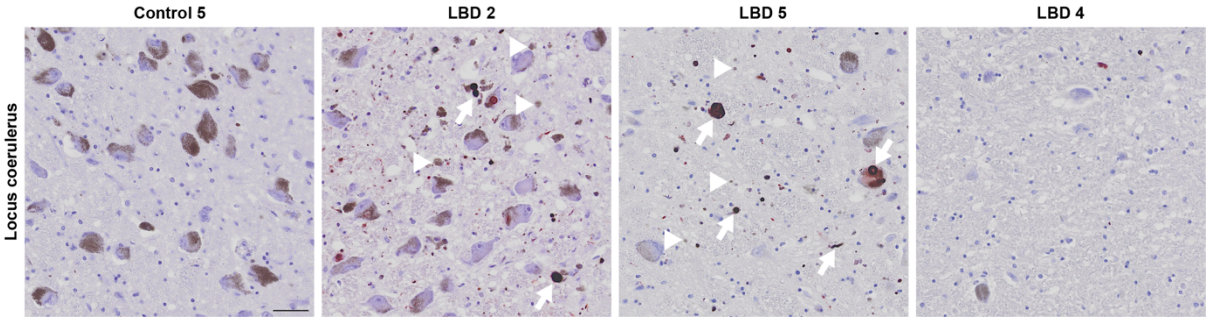

Fig. 7 Cell loss and extra-neuronal neuromelanin in the locus coeruleus of LBD cases

Locus coeruleus displayed varying degrees of loss of its noradrenergic, neuromelanin-containing neurons in the LBD cases, as illustrated with a progressive fall in the density of melanized neurons (left to right). Extra-neuronal neuromelanin was apparent in some cases (arrowheads in LBD 2 and 5), evincing neuronal loss. PLA signal density was also lower in LBD cases with extensive neuronal loss (arrows indicate examples of Lewy-like PLA). Scale bar = 50 µm.

Discussion

In recent years, several studies have demonstrated previously undetected α-synuclein aggregate pathology not organised into LBs in PD, DLB, and multiple system atrophy (MSA) using α-synuclein PLA [31, 51, 60, 61]. With their signal amplification creating a high signal-to-noise ratio, the PLAs are capable of detecting aggregate species with low epitope density, which enables detection of, e.g., α-synuclein oligomers. In the present study, we used a variation of the recently published MJF-14 PLA [31], which labels both inclusions of Lewy-type morphology as well as the non-inclusion aggregates. With this assay, we present the first evidence of a broad accumulation of α-synuclein aggregates not organised into inclusions in multiple brain regions of LRRK2 cases without LBs. Of the six cases examined, five of them presented with significant particulate PLA signal in all the five brain regions examined, but the exact distribution and density differed between the various cases and brain regions investigated.

Curiously, several of the LRRK2 cases did not show particularly dense PLA staining in the brainstem regions such as DMV, LC, and SNpc. Instead, we detected a particular affection of inferior olivary and pontine nuclei as well as pontocerebellar fibres, raising the speculation whether this is a general feature of LRRK2 cases. These regions are generally implicated in MSA rather than the LBDs, though sparse Lewy pathology has been reported in some PD and DLB cases [59, 67]. If this observation is shown to be a common characteristic in LRRK2-mutant cases, it may suggest a slight cerebellar dysfunction in these patients, which should then be investigated clinically. In general, the LRRK2 cases presented with a higher degree of particulate PLA signal than both the regular LBD cases and the non-neurodegenerative controls, though one LBD case did show particulate PLA signal at levels similar to most of the LRRK2 cases.

The striking prevalence of particulate PLA in the LRRK2 cases suggests that their lack of LBs does not reflect an absence of α-synuclein aggregate pathology but rather an inability to form the characteristic inclusions. Though knowledge of the mechanisms involved in LB formation is limited, LBs are clearly complex structures, and their formation appears to be a specific cellular response, which might indeed be perturbed in some cases [16, 35, 38, 44, 62, 64, 66]. LRRK2 has mechanistically been associated

with vesicular trafficking and autophagy, and mutation-associated perturbations of proteostasis could thus represent a link to the absence of LBs [24, 37, 55]. However, since the absence of LBs is not linked to any specific LRRK2-mutation and varies even within the same family, LRRK2 is not the sole player in the perturbation of LB formation [33, 48, 72]. Consequently, further studies to determine whether such non-inclusion α-synuclein aggregate pathology is a general feature of PD patients with mutations in LRRK2 or in Parkin (PRKN), who also frequently present without LBs, are strongly motivated [15].

Curiously, a recent study using α-synuclein seed amplification assay (SAA) on more than 1100 participants in the Parkinson's Progression Marker Initiative (PPMI) cohort showed that SAA-positivity was significantly lower among LRRK2 PD than idiopathic PD patients [63]. At the time of the study, neuropathological examination was only available for a small subset of cases, including one SAA-negative LRRK2 carrier, who did not contain Lewy pathology. In contrast, all cases with a positive SAA showed typical Lewy pathology upon neuropathological examination [63]. At present, the correlation between SAA-positivity and presence of α-synuclein PLA signal has not been studied, though such studies would be strongly motivated. A recent study, however, did examine the relation between SAA-positivity and regional presence of Lewy pathology, demonstrating significantly lower SAA-positivity in cases with early (Braak stages 1-3) or focal pathology (e.g., amygdala-predominant) [4]. Moreover, they found SAA-positivity in brain homogenates from multiple brain regions without accompanying Lewy pathology, indicating a seeding activity of smaller or less organized α-synuclein aggregates [4]. As such, the lack of SAA-positivity in some of the LRRK2 cases in the PPMI cohort does not necessarily constitute no α-synuclein pathology but could also be caused by predominantly focal pathology, which is not reflected in the cerebrospinal fluid. Alternatively, pathology consisting of non-inclusion (presumably oligomeric) α-synuclein may have a lower seeding efficiency than mature α-synuclein fibrils in the SAA, in line with evidence from experimental models [39, 46]. Regardless, inclusion of α-synuclein PLA staining of post-mortem cases in the coming follow-up studies on the PPMI cohort should aid in our understanding of the LRRK2-related PD neuropathology.

Multiple studies examining LRRK2 carriers (see Suppl. Table 2 for comprehensive list) have shown that LB-negative cases display Alzheimer's disease (AD) or PSP-like tau pathology or show unspecific nigral cell loss without any underlying pathology [6, 28, 54, 65, 69, 72]. However, other pleiomorphic pathologies also include MSA and argyrophilic grain disease [27, 50]. Except for the PSP-diagnosed LRRK2 4, which was confirmed by neuropathology, only two of the LRRK2 cases in this cohort (LRRK2 1 and 4) displayed low-grade AD-like tau pathology. This finding is somewhat contrasting with the findings from Henderson et al. who examined a cohort of 11 LRRK2 cases, of which four were LB-negative [28]. These cases, mostly with G2019S mutation, all contained AD-like tau pathology, though levels in LB-negative cases tended to be lower than in the LB-positive cases [28]. Whether the divergent neuropathological findings are related to specific LRRK2 mutations is yet to be determined in larger cohort studies.

For most of the healthy control cases, stained in parallel with LRRK2 and regular LBD cases, only very low levels of particulate PLA were detected. None of the healthy controls showed any LBs or other neurodegenerative proteinaceous inclusions, such as Aβ plaques and tau tangles. Two of the controls (Control 2 and 6), however, did present with higher levels of particulate PLA, which were closer to the levels seen in some of the LBD and LRRK2 cases. This was seen particularly in the amygdala and SNpc but not in DMV or LC, which are usually thought to be affected early on with Lewy-like pathology. Previous studies using α-synuclein PLA have shown that it appears to detect earlier aggregate species

than the Lewy pathology [31, 51, 61]. These two controls could thus represent early asymptomatic stages of LBD, perhaps of the brain-first subtype[7, 29, 30], that would have become symptomatic, had they lived longer. As we did have two other controls (Control 4 and 5) that were virtually void of any PLA signal in the study, it is unlikely that the α-synuclein PLA accumulation is a normal, disease-unrelated process. Whether there is a certain threshold above which the PLA-positive species become problematic and how they progress in the brain is currently unknown and requires further studies in larger, aged cohorts.

The main limitation of this study pertains to the relatively small cohort size, which relates to the scarcity of LB-negative LRRK2 cases available for post-mortem examination. As such, larger studies are needed to determine whether the non-inclusion α-synuclein aggregate pathology is a general feature of LRRK2 cases and how its extent and distribution may correlate with other protein pathologies. Additionally, the inclusion of cases with different clinical diagnoses (in both LRRK2 and LBD groups) could obscure features that are specific for one clinical diagnosis but were not apparent in our study due to group heterogeneity. Nevertheless, we here provide compelling evidence that Lewy pathology is not representative of all α-synuclein aggregation in the brain.

In conclusion, we here provide evidence of substantial α-synuclein aggregate pathology, but no Lewy-like neuritic or somatic inclusions, in LB-negative LRRK2 cases. The particulate PLA affects both classical PD-related brain regions in the LRRK2 cases, but also other regions not usually implicated in PD, particularly the inferior olivary nucleus and the pontocerebellar pathways. These results motivate further studies on not only LRRK2 cases but also PRKN PD cases, which also frequently present without LBs upon autopsy. Furthermore, we need to also examine larger aged cohorts to understand how this particulate PLA signal progresses in the brain and when it becomes associated to clinical symptoms.

Data availability

All data are presented in the manuscript or the supplementary material. Raw data supporting the findings of this study are available from the corresponding author upon reasonable request.

Acknowledgements

The authors would like to sincerely thank all the brain donors for their contribution to this research. We acknowledge the Oxford Brain Bank, supported by the Medical Research Council (MRC), Brains for Dementia Research (BDR) (Alzheimer Society and Alzheimer Research UK), and the NIHR Oxford Biomedical Research Centre, as well as Imperial Brain Bank supported by Parkinson's UK for supplying tissue. We further acknowledge the Imaging Core at the Department of Biomedicine, Aarhus University, for the use of facilities and assistance in imaging.

Funding

This study was supported by the following funding sources: Michael J Fox Foundation for Parkinson's Research for PHJ (grant ID 12028.01); Lundbeck Foundation (grants R223-2015-4222 for PHJ and R248-2016-2518 for Danish Research Institute of Translational Neuroscience – DANDRITE, Nordic-EMBL Partnership for Molecular Medicine, Aarhus University, Denmark); The Danish Parkinson Association for PHJ; Bjarne Saxhof Foundation for PHJ; Aarhus University Graduate School of Health PhD Fellow

grant for NMJ. Additionally, LP is supported by the GSK-Institute of Molecular and Computational Medicine, National Institute for Health Research (NIHR), Oxford Biomedical Research Centre (BRC), Parkinson Foundation, Michael J Fox Foundation for Parkinson's Research, and the National Institute of Health.

Author information

Author affiliations

DANDRITE - Danish Research Institute of Translational Neuroscience, Aarhus C, Denmark.

Nanna Møller Jensen, Zagorka Vitic, Mia R. Antorini, Tobias Bruun Viftrup, Poul Henning Jensen.

Department of Biomedicine, Aarhus University, Aarhus C, Denmark.

Nanna Møller Jensen, Zagorka Vitic, Mia R. Antorini, Tobias Bruun Viftrup, Poul Henning Jensen.

Oxford Parkinson's Disease Centre, University of Oxford, Oxford, United Kingdom.
Laura Parkkinen.

Nuffield Department of Clinical Neurosciences, University of Oxford, Oxford, United Kingdom.
Laura Parkkinen.

Author contributions

NMJ, LP, and PHJ conceived and designed the study, and LP obtained post-mortem brain samples. NMJ, ZV, MRA, and TBV performed the experiments and analysed the data, while LP and PHJ provided critical input for the interpretation of data. Figures and first draft of the manuscript were prepared by NMJ. All authors provided feedback and approved the final version of the manuscript.

Ethics declarations

Conflicts of interest

The authors have no relevant financial or non-financial conflicts of interest to disclose.

Ethical approval and informed consent

Post-mortem brain tissue was obtained from Parkinson's UK Brain Bank (PUKBB), Imperial College London, and Oxford Brain Bank (OBB), Nuffield Department of Clinical Neurosciences in University of Oxford, in accordance with approved protocols by the Wales Research Ethics Committee (23/WA/0273) and the Ethics Committee of the University of Oxford (ref 23/SC/0241). All participants had given prior written informed consent for the brain donation. Both brain banks comply with the requirements of the Human Tissue Act 2004 and the Codes of Practice set by the Human Tissue Authority (HTA licence numbers 12275 for PUKBB and 12217 for OBB).

References

1. Amunts K, Kedo O, Kindler M, Pieperhoff P, Mohlberg H, Shah NJ, Habel U, Schneider F, Zilles K (2005) Cytoarchitectonic mapping of the human amygdala, hippocampal region and entorhinal cortex: Intersubject variability and probability maps. Anat Embryol (Berl) 210:343–352. doi: 10.1007/S00429-005-0025-5/FIGURES/4
2. Bankhead P, Loughrey MB, Fernández JA, Dombrowski Y, McArt DG, Dunne PD, McQuaid S, Gray RT, Murray LJ, Coleman HG, James JA, Salto-Tellez M, Hamilton PW (2017) QuPath: Open source software for digital pathology image analysis. Scientific Reports 2017 7:1 7:1–7. doi: 10.1038/s41598-017-17204-5
3. Beach TG, Adler CH, Lue LF, Sue LI, Bachalakuri J, Henry-Watson J, Sasse J, Boyer S, Shirohi S, Brooks R, Eschbacher J, White CL, Akiyama H, Caviness J, Shill HA, Connor DJ, Sabbagh MN, Walker DG (2009) Unified staging system for Lewy body disorders: Correlation with nigrostriatal degeneration, cognitive impairment and motor dysfunction. Acta Neuropathol 117:613–634. doi: 10.1007/s00401-009-0538-8
4. Bentivenga GM, Mammana A, Baiardi S, Rossi M, Ticca A, Magliocchetti F, Mastrangelo A, Poleggi A, Ladogana A, Capellari S, Parchi P (2024) Performance of a seed amplification assay for misfolded alpha-synuclein in cerebrospinal fluid and brain tissue in relation to Lewy body disease stage and pathology burden. Acta Neuropathol 147:1–13. doi: 10.1007/S00401-023-02663-0/FIGURES/4
5. Berwick DC, Heaton GR, Azeggagh S, Harvey K (2019) LRRK2 Biology from structure to dysfunction: research progresses, but the themes remain the same. Molecular Neurodegeneration 2019 14:1 14:1–22. doi: 10.1186/S13024-019-0344-2
6. Blauwendraat C, Pletnikova O, Geiger JT, Murphy NA, Abramzon Y, Rudow G, Mamais A, Sabir MS, Crain B, Ahmed S, Rosenthal LS, Bakker CC, Faghri F, Chia R, Ding J, Dawson TM, Pantelyat A, Albert MS, Nalls MA, Resnick SM, Ferrucci L, Cookson MR, Hillis AE, Troncoso JC, Scholz SW (2019) Genetic analysis of neurodegenerative diseases in a pathology cohort. Neurobiol Aging 76:214.e1-214.e9. doi: 10.1016/J.NEUROBIOLAGING.2018.11.007
7. Borghammer P, Horsager J, Andersen K, Van Den Berge N, Raunio A, Murayama S, Parkkinen L, Myllykangas L (2021) Neuropathological evidence of body-first vs. brain-first Lewy body disease. Neurobiol Dis 161:105557. doi: 10.1016/j.nbd.2021.105557
8. Braak H, Ghebremedhin E, Rüb U, Bratzke H, Del Tredici K (2004) Stages in the development of Parkinson's disease-related pathology. Cell Tissue Res 318:121–134
9. Braak H, Del Tredici K, Rüb U, De Vos RAI, Jansen Steur ENH, Braak E (2003) Staging of brain pathology related to sporadic Parkinson's disease. Neurobiol Aging 24:197–211. doi: 10.1016/S0197-4580(02)00065-9
10. Cherian A, Divya KP (2020) Genetics of Parkinson's disease. Acta Neurol Belg 120:1297–1305. doi: 10.1007/S13760-020-01473-5/TABLES/1
11. Covy JP, Yuan W, Waxman EA, Hurtig HI, Van Deerlin VM, Giasson BI (2009) Clinical and pathological characteristics of patients with Leucine-rich repeat kinase-2 mutations. Movement Disorders 24:32–39. doi: 10.1002/MDS.22096
12. Dächsel JC, Ross OA, Mata IF, Kachergus J, Toft M, Cannon A, Baker M, Adamson J, Hutton M, Dickson DW, Farrer MJ (2007) Lrrk2 G2019S substitution in frontotemporal lobar degeneration with ubiquitin-immunoreactive neuronal inclusions. Acta Neuropathol 113:601–606. doi: 10.1007/S00401-006-0178-1/FIGURES/1

13. Day JO, Mullin S (2021) The Genetics of Parkinson's Disease and Implications for Clinical Practice. Genes 2021, Vol 12, Page 1006 12:1006. doi: 10.3390/GENES12071006
14. Dickson DW, Braak H, Duda JE, Duyckaerts C, Gasser T, Halliday GM, Hardy J, Leverenz JB, Del Tredici K, Wszolek ZK, Litvan I (2009) Neuropathological assessment of Parkinson's disease: refining the diagnostic criteria. Lancet Neurol 8:1150–1157
15. Doherty KM, Silveira-Moriyama L, Parkkinen L, Healy DG, Farrell M, Mencacci NE, Ahmed Z, Brett FM, Hardy J, Quinn N, Counihan TJ, Lynch T, Fox Z V., Revesz T, Lees AJ, Holton JL (2013) Parkin Disease: A Clinicopathologic Entity? JAMA Neurol 70:571–579. doi: 10.1001/JAMANEUROL.2013.172
16. Duffy PE, Tennyson VM (1965) Phase and Electron Microscopic Observations of Lewy Bodies and Melanin Granules in the Substantia Nigra and Locus Caeruleus in Parkinson's Disease. J Neuropathol Exp Neurol 24:398–414. doi: 10.1097/00005072-196507000-00003
17. Gai WP, Blumbergs PC, Geffen LB, Blessing WW (1992) Age-related loss of dorsal vagal neurons in Parkinson's disease. Neurology 42:2106–2111. doi: 10.1212/WNL.42.11.2106
18. Gaig C, Martí MJ, Ezquerra M, Rey MJ, Cardozo A, Tolosa E (2007) G2019S LRRK2 mutation causing Parkinson's disease without Lewy bodies. J Neurol Neurosurg Psychiatry 78:626–628. doi: 10.1136/JNNP.2006.107904
19. German DC, Manaye KF, White CL, Woodward DJ, McIntire DD, Smith WK, Kalaria RN, Mann DMA (1992) Disease-specific patterns of locus coeruleus cell loss. Ann Neurol 32:667–676. doi: 10.1002/ANA.410320510
20. Giasson BI, Covy JP, Bonini NM, Hurtig HI, Farrer MJ, Trojanowski JQ, Van Deerlin VM (2006) Biochemical and pathological characterization of Lrrk2. Ann Neurol 59:315–322. doi: 10.1002/ANA.20791
21. Gilks WP, Abou-Sleiman PM, Gandhi S, Jain S, Singleton A, Lees AJ, Shaw K, Bhatia KP, Bonifati V, Quinn NP, Lynch J, Healy DG, Holton JL, Revesz T, Wood NW (2005) A common LRRK2 mutation in idiopathic Parkinson's disease. The Lancet 365:415–416. doi: 10.1016/S0140-6736(05)17830-1
22. Giordana MT, D'Agostino C, Albani G, Mauro A, Di Fonzo A, Antonini A, Bonifati V (2007) Neuropathology of Parkinson's disease associated with the LRRK2 Ile1371Val mutation. Movement Disorders 22:275–278. doi: 10.1002/MDS.21281
23. Gomez A, Ferrer I (2010) Involvement of the cerebral cortex in Parkinson disease linked with G2019S LRRK2 mutation without cognitive impairment. Acta Neuropathol 120:155–167. doi: 10.1007/S00401-010-0669-Y
24. Gómez-Suaga P, Luzón-Toro B, Churamani D, Zhang L, Bloor-Young D, Patel S, Woodman PG, Churchill GC, Hilfiker S (2012) Leucine-rich repeat kinase 2 regulates autophagy through a calcium-dependent pathway involving NAADP. Hum Mol Genet 21:511–525. doi: 10.1093/HMG/DDR481
25. Halliday G, Reyes S, Double K (2012) Substantia Nigra, Ventral Tegmental Area, and Retrorubral Fields. The Human Nervous System, Third Edition 439–455. doi: 10.1016/B978-0-12-374236-0.10013-6
26. Harding AJ, Halliday GM (2001) Cortical Lewy body pathology in the diagnosis of dementia. Acta Neuropathol 102:355–363. doi: 10.1007/S004010100390
27. Hasegawa K, Stoessl AJ, Yokoyama T, Kowa H, Wszolek ZK, Yagishita S (2009) Familial parkinsonism: study of original Sagamihara PARK8 (I2020T) kindred with variable

clinicopathologic outcomes. Parkinsonism Relat Disord 15:300–306. doi: 10.1016/J.PARKRELDIS.2008.07.010
28. Henderson MX, Sengupta M, Trojanowski JQ, Lee VMY (2019) Alzheimer's disease tau is a prominent pathology in LRRK2 Parkinson's disease. Acta Neuropathol Commun 7:183. doi: 10.1186/s40478-019-0836-x
29. Horsager J, Andersen KB, Knudsen K, Skjærbæk C, Fedorova TD, Okkels N, Schaeffer E, Bonkat SK, Geday J, Otto M, Sommerauer M, Danielsen EH, Bech E, Kraft J, Munk OL, Hansen SD, Pavese N, Göder R, Brooks DJ, Berg D, Borghammer P (2020) Brain-first versus body-first Parkinson's disease: A multimodal imaging case-control study. Brain 143:3077–3088. doi: 10.1093/brain/awaa238
30. Horsager J, Borghammer P (2024) Brain-first vs. body-first Parkinson's disease: An update on recent evidence. Parkinsonism Relat Disord 122:106101
31. Jensen NM, Fu Y, Betzer C, Li H, Elfarrash S, Shaib AH, Krah D, Vitic Z, Reimer L, Gram H, Buchman V, Denham M, Rizzoli SO, Halliday GM, Jensen PH (2024) MJF-14 proximity ligation assay detects early non-inclusion alpha-synuclein pathology with enhanced specificity and sensitivity. NPJ Parkinsons Dis 10:227. doi: 10.1038/s41531-024-00841-9
32. Kalia L V, Lang AE (2015) Parkinson's disease. The Lancet 386:896–912. doi: 10.1016/S0140-6736(14)61393-3
33. Kalia L V., Lang AE, Hazrati LN, Fujioka S, Wszolek ZK, Dickson DW, Ross OA, Van Deerlin VM, Trojanowski JQ, Hurtig HI, Alcalay RN, Marder KS, Clark LN, Gaig C, Tolosa E, Ruiz-Martínez J, Marti-Masso JF, Ferrer I, López De Munain A, Goldman SM, Schüle B, Langston JW, Aasly JO, Giordana MT, Bonifati V, Puschmann A, Canesi M, Pezzoli G, Maues De Paula A, Hasegawa K, Duyckaerts C, Brice A, Stoessl AJ, Marras C (2015) Clinical Correlations With Lewy Body Pathology in LRRK2-Related Parkinson Disease. JAMA Neurol 72:100–105. doi: 10.1001/JAMANEUROL.2014.2704
34. Khan NL, Jain S, Lynch JM, Pavese N, Abou-Sleiman P, Holton JL, Healy DG, Gilks WP, Sweeney MG, Ganguly M, Gibbons V, Gandhi S, Vaughan J, Eunson LH, Katzenschlager R, Gayton J, Lennox G, Revesz T, Nicholl D, Bhatia KP, Quinn N, Brooks D, Lees AJ, Davis MB, Piccini P, Singleton AB, Wood NW (2005) Mutations in the gene LRRK2 encoding dardarin (PARK8) cause familial Parkinson's disease: clinical, pathological, olfactory and functional imaging and genetic data. Brain 128:2786–2796. doi: 10.1093/BRAIN/AWH667
35. Lashuel HA (2020) Do Lewy bodies contain alpha-synuclein fibrils? and Does it matter? A brief history and critical analysis of recent reports. Neurobiol Dis 141:104876
36. Ling H, Kara E, Bandopadhyay R, Hardy J, Holton J, Xiromerisiou G, Lees A, Houlden H, Revesz T (2013) TDP-43 pathology in a patient carrying G2019S LRRK2 mutation and a novel p.Q124E MAPT. Neurobiol Aging 34:2889.e5-2889.e9. doi: 10.1016/J.NEUROBIOLAGING.2013.04.011
37. Madureira M, Connor-Robson N, Wade-Martins R (2020) "LRRK2: Autophagy and Lysosomal Activity." Front Neurosci 14:536324. doi: 10.3389/FNINS.2020.00498/BIBTEX
38. Mahul-Mellier AL, Burtscher J, Maharjan N, Weerens L, Croisier M, Kuttler F, Leleu M, Knott GW, Lashuel HA (2020) The process of Lewy body formation, rather than simply α-synuclein fibrillization, is one of the major drivers of neurodegeneration. Proc Natl Acad Sci U S A 117:4971–4982. doi: 10.1073/pnas.1913904117

39. Mahul-Mellier AL, Vercruysse F, MacO B, Ait-Bouziad N, De Roo M, Muller D, Lashuel HA (2015) Fibril growth and seeding capacity play key roles in α-synuclein-mediated apoptotic cell death. Cell Death Differ 22:2107–2122. doi: 10.1038/cdd.2015.79
40. Martí-Massó JF, Ruiz-Martínez J, Bolaño MJ, Ruiz I, Gorostidi A, Moreno F, Ferrer I, López De Munain A (2009) Neuropathology of Parkinson's disease with the R1441G mutation in LRRK2. Mov Disord 24:1998–2001. doi: 10.1002/MDS.22677
41. McKeith IG, Boeve BF, Dickson DW, Halliday G, Taylor JP, Weintraub D, Aarsland D, Galvin J, Attems J, Ballard CG, Bayston A, Beach TG, Blanc F, Bohnen N, Bonanni L, Bras J, Brundin P, Burn D, Chen-Plotkin A, Duda JE, El-Agnaf O, Feldman H, Ferman TJ, Ffytche D, Fujishiro H, Galasko D, Goldman JG, Gomperts SN, Graff-Radford NR, Honig LS, Iranzo A, Kantarci K, Kaufer D, Kukull W, Lee VMY, Leverenz JB, Lewis S, Lippa C, Lunde A, Masellis M, Masliah E, McLean P, Mollenhauer B, Montine TJ, Moreno E, Mori E, Murray M, O'Brien JT, Orimo S, Postuma RB, Ramaswamy S, Ross OA, Salmon DP, Singleton A, Taylor A, Thomas A, Tiraboschi P, Toledo JB, Trojanowski JQ, Tsuang D, Walker Z, Yamada M, Kosaka K (2017) Diagnosis and management of dementia with Lewy bodies. Neurology 89:88–100
42. Mulroy E, Erro R, Bhatia KP, Hallett M (2024) Refining the clinical diagnosis of Parkinson's disease. Parkinsonism Relat Disord 122
43. Nakano I, Hirano A (1984) Parkinson's disease: neuron loss in the nucleus basalis without concomitant Alzheimer's disease. Ann Neurol 15:415–418. doi: 10.1002/ANA.410150503
44. Olanow CW, Perl DP, DeMartino GN, McNaught KSP (2004) Lewy-body formation is an aggresome-related process: A hypothesis. Lancet Neurology 3:496–503
45. Outeiro TF, Koss DJ, Erskine D, Walker L, Kurzawa-Akanbi M, Burn D, Donaghy P, Morris C, Taylor JP, Thomas A, Attems J, McKeith I (2019) Dementia with Lewy bodies: An update and outlook. Mol Neurodegener 14:1–18
46. Pieri L, Madiona K, Melki R (2016) Structural and functional properties of prefibrillar α-synuclein oligomers. Sci Rep 6:1–15. doi: 10.1038/srep24526
47. Polymeropoulos MH (1997) Mutation in the α-Synuclein Gene Identified in Families with Parkinson's Disease. Science (1979) 276:2045–2047. doi: 10.1126/science.276.5321.2045
48. Poulopoulos M, Levy OA, Alcalay RN (2012) The neuropathology of genetic Parkinson's disease. Movement Disorders 27:831–842. doi: 10.1002/MDS.24962
49. Puschmann A, Englund E, Ross OA, Vilariño-Güell C, Lincoln SJ, Kachergus JM, Cobb SA, Törnqvist AL, Rehncrona S, Widner H, Wszolek ZK, Farrer MJ, Nilsson C (2012) First neuropathological description of a patient with Parkinson's disease and LRRK2 p.N1437H mutation. Parkinsonism Relat Disord 18:332–338. doi: 10.1016/J.PARKRELDIS.2011.11.019
50. Rajput A, Dickson DW, Robinson CA, Ross OA, Dächsel JC, Lincoln SJ, Cobb SA, Rajput ML, Farrer MJ (2006) Parkinsonism, Lrrk2 G2019S, and tau neuropathology. Neurology 67:1506–1508. doi: 10.1212/01.WNL.0000240220.33950.0C
51. Roberts RF, Wade-Martins R, Alegre-Abarrategui J (2015) Direct visualization of alpha-synuclein oligomers reveals previously undetected pathology in Parkinson's disease brain. Brain 138:1642–1657. doi: 10.1093/brain/awv040
52. Ross OA, Toft M, Whittle AJ, Johnson JL, Papapetropoulos S, Mash DC, Litvan I, Gordon MF, Wszolek ZK, Farrer MJ, Dickson DW (2006) Lrrk2 and Lewy body disease. Ann Neurol 59:388–393. doi: 10.1002/ANA.20731

53. Ruffmann C, Giaccone G, Canesi M, Bramerio M, Goldwurm S, Gambacorta M, Rossi G, Tagliavini F, Pezzoli G (2012) Atypical tauopathy in a patient with LRRK2-G2019S mutation and tremor-dominant Parkinsonism. Neuropathol Appl Neurobiol 38:382–386. doi: 10.1111/J.1365-2990.2011.01216.X
54. Sanchez-Contreras M, Heckman MG, Tacik P, Diehl N, Brown PH, Soto-Ortolaza AI, Christopher EA, Walton RL, Ross OA, Golbe LI, Graff-Radford N, Wszolek ZK, Dickson DW, Rademakers R (2017) Study of LRRK2 variation in tauopathy: Progressive supranuclear palsy and corticobasal degeneration. Movement Disorders 32:115–123. doi: 10.1002/MDS.26815
55. Schapansky J, Khasnavis S, DeAndrade MP, Nardozzi JD, Falkson SR, Boyd JD, Sanderson JB, Bartels T, Melrose HL, LaVoie MJ (2018) Familial knockin mutation of LRRK2 causes lysosomal dysfunction and accumulation of endogenous insoluble α-synuclein in neurons. Neurobiol Dis 111:26–35. doi: 10.1016/J.NBD.2017.12.005
56. Schapira AHV, Chaudhuri KR, Jenner P (2017) Non-motor features of Parkinson disease. Nature Reviews Neuroscience 2017 18:7 18:435–450. doi: 10.1038/nrn.2017.62
57. Schneider SA, Alcalay RN (2017) Neuropathology of genetic synucleinopathies with parkinsonism: Review of the literature. Movement Disorders 32:1504–1523. doi: 10.1002/MDS.27193
58. Schröder H, de Vos RAI, Huggenberger S, Müller-Thomsen L, Rozemuller A, Hedayat F, Moser N (2023) Histology atlas of the human brainstem. In: The Human Brainstem. Springer, Cham, pp 539–630
59. Seidel K, Mahlke J, Siswanto S, Krüger R, Heinsen H, Auburger G, Bouzrou M, Grinberg LT, Wicht H, Korf HW, Den Dunnen W, Rüb U (2015) The Brainstem Pathologies of Parkinson's Disease and Dementia with Lewy Bodies. Brain Pathology 25:121–135. doi: 10.1111/BPA.12168
60. Sekiya H, Kowa H, Koga H, Takata M, Satake W, Futamura N, Funakawa I, Jinnai K, Takahashi M, Kondo T, Ueno Y, Kanagawa M, Kobayashi K, Toda T (2019) Wide distribution of alpha-synuclein oligomers in multiple system atrophy brain detected by proximity ligation. Acta Neuropathol 137:455–466. doi: 10.1007/s00401-019-01961-w
61. Sekiya H, Tsuji A, Hashimoto Y, Takata M, Koga S, Nishida K, Futamura N, Kawamoto M, Kohara N, Dickson DW, Kowa H, Toda T (2022) Discrepancy between distribution of alpha-synuclein oligomers and Lewy-related pathology in Parkinson's disease. Acta Neuropathol Commun 10:133. doi: 10.1186/s40478-022-01440-6
62. Shahmoradian SH, Lewis AJ, Genoud C, Hench J, Moors TE, Navarro PP, Castaño-Díez D, Schweighauser G, Graff-Meyer A, Goldie KN, Sütterlin R, Huisman E, Ingrassia A, Gier Y de, Rozemuller AJM, Wang J, Paepe A De, Erny J, Staempfli A, Hoernschemeyer J, Großerüschkamp F, Niedieker D, El-Mashtoly SF, Quadri M, Van IJcken WFJ, Bonifati V, Gerwert K, Bohrmann B, Frank S, Britschgi M, Stahlberg H, Van de Berg WDJ, Lauer ME (2019) Lewy pathology in Parkinson's disease consists of crowded organelles and lipid membranes. Nature Neuroscience 2019 22:7 22:1099–1109. doi: 10.1038/s41593-019-0423-2
63. Siderowf A, Concha-Marambio L, Lafontant DE, Farris CM, Ma Y, Urenia PA, Nguyen H, Alcalay RN, Chahine LM, Foroud T, Galasko D, Kieburtz K, Merchant K, Mollenhauer B, Poston KL, Seibyl J, Simuni T, Tanner CM, Weintraub D, Videnovic A, Choi SH, Kurth R, Caspell-Garcia C, Coffey CS, Frasier M, Oliveira LMA, Hutten SJ, Sherer T, Marek K,

Soto C (2023) Assessment of heterogeneity among participants in the Parkinson's Progression Markers Initiative cohort using α-synuclein seed amplification: a cross-sectional study. Lancet Neurol 22:407–417. doi: 10.1016/S1474-4422(23)00109-6

64. Trinkaus VA, Riera-Tur I, Martínez-Sánchez A, Bäuerlein FJB, Guo Q, Arzberger T, Baumeister W, Dudanova I, Hipp MS, Hartl FU, Fernández-Busnadiego R (2021) In situ architecture of neuronal α-Synuclein inclusions. Nature Communications 2021 12:1 12:1–10. doi: 10.1038/s41467-021-22108-0
65. Ujiie S, Hatano T, Kubo SI, Imai S, Sato S, Uchihara T, Yagishita S, Hasegawa K, Kowa H, Sakai F, Hattori N (2012) LRRK2 I2020T mutation is associated with tau pathology. Parkinsonism Relat Disord 18:819–823. doi: 10.1016/J.PARKRELDIS.2012.03.024
66. Wakabayashi K, Tanji K, Mori F, Takahashi H (2007) The Lewy body in Parkinson's disease: Molecules implicated in the formation and degradation of α-synuclein aggregates. In: Neuropathology. John Wiley & Sons, Ltd (10.1111), pp 494–506
67. Wenning GK, Tison F, Elliott L, Quinn NP, Daniel SE (1996) Olivopontocerebellar pathology in multiple system atrophy. Mov Disord 11:157–162. doi: 10.1002/MDS.870110207
68. Woolsey TA, Hanaway J, Gado MH (2017) The Brain Atlas: A Visual Guide to the Human Central Nervous System, 3rd Edition, 4th ed
69. Wszolek ZK, Pfeiffer RF, Tsuboi Y, Uitti RJ, McComb RD, Stoessl AJ, Strongosky AJ, Zimprich A, Müller-Myhsok B, Farrer MJ, Gasser T, Calne DB, Dickson DW (2004) Autosomal dominant parkinsonism associated with variable synuclein and tau pathology. Neurology 62:1619–1622. doi: 10.1212/01.WNL.0000125015.06989.DB
70. Wszolek ZK, Vieregge P, Uitti RJ, Gasser T, Yasuhara O, McGeer P, Berry K, Calne DB, Vingerhoets FJG, Klein C, Pfeiffer RF (1997) German-Canadian family (Family A) with Parkinsonism, Amyotrophy, and Dementia-longitudinal observations. Parkinsonism Relat Disord 3:125–139. doi: 10.1016/S1353-8020(97)00013-8
71. Yilmazer-Hanke DM, Wolf HK, Schramm J, Elger CE, Wiestler OD, Blümcke I (2000) Subregional Pathology of the Amygdala Complex and Entorhinal Region in Surgical Specimens From Patients With Pharmacoresistant Temporal Lobe Epilepsy. J Neuropathol Exp Neurol 59
72. Zimprich A, Biskup S, Leitner P, Lichtner P, Farrer M, Lincoln S, Kachergus J, Hulihan M, Uitti RJ, Calne DB, Stoessl AJ, Pfeiffer RF, Patenge N, Carbajal IC, Vieregge P, Asmus F, Müller-Myhsok B, Dickson DW, Meitinger T, Strom TM, Wszolek ZK, Gasser T (2004) Mutations in LRRK2 Cause Autosomal-Dominant Parkinsonism with Pleomorphic Pathology. Neuron 44:601–607. doi: 10.1016/J.NEURON.2004.11.005

Supplementary material for the study

Abundant non-inclusion α-synuclein pathology in Lewy body-negative LRRK2-mutant cases

Nanna Møller Jensen[1,2,*], Zagorka Vitic[1,2], Mia R. Antorini[1,2], Tobias Bruun Viftrup[1,2], Laura Parkkinen[3,4,#,*], Poul Henning Jensen[1,2,#,*]

[1]DANDRITE - Danish Research Institute of Translational Neuroscience, Aarhus C, Denmark.
[2]Department of Biomedicine, Aarhus University, Aarhus C, Denmark.
[3]Oxford Parkinson's Disease Centre, University of Oxford, Oxford, United Kingdom.
[4]Nuffield Department of Clinical Neurosciences, University of Oxford, Oxford, United Kingdom.
[#]These authors are shared last author.
*These authors are corresponding authors.

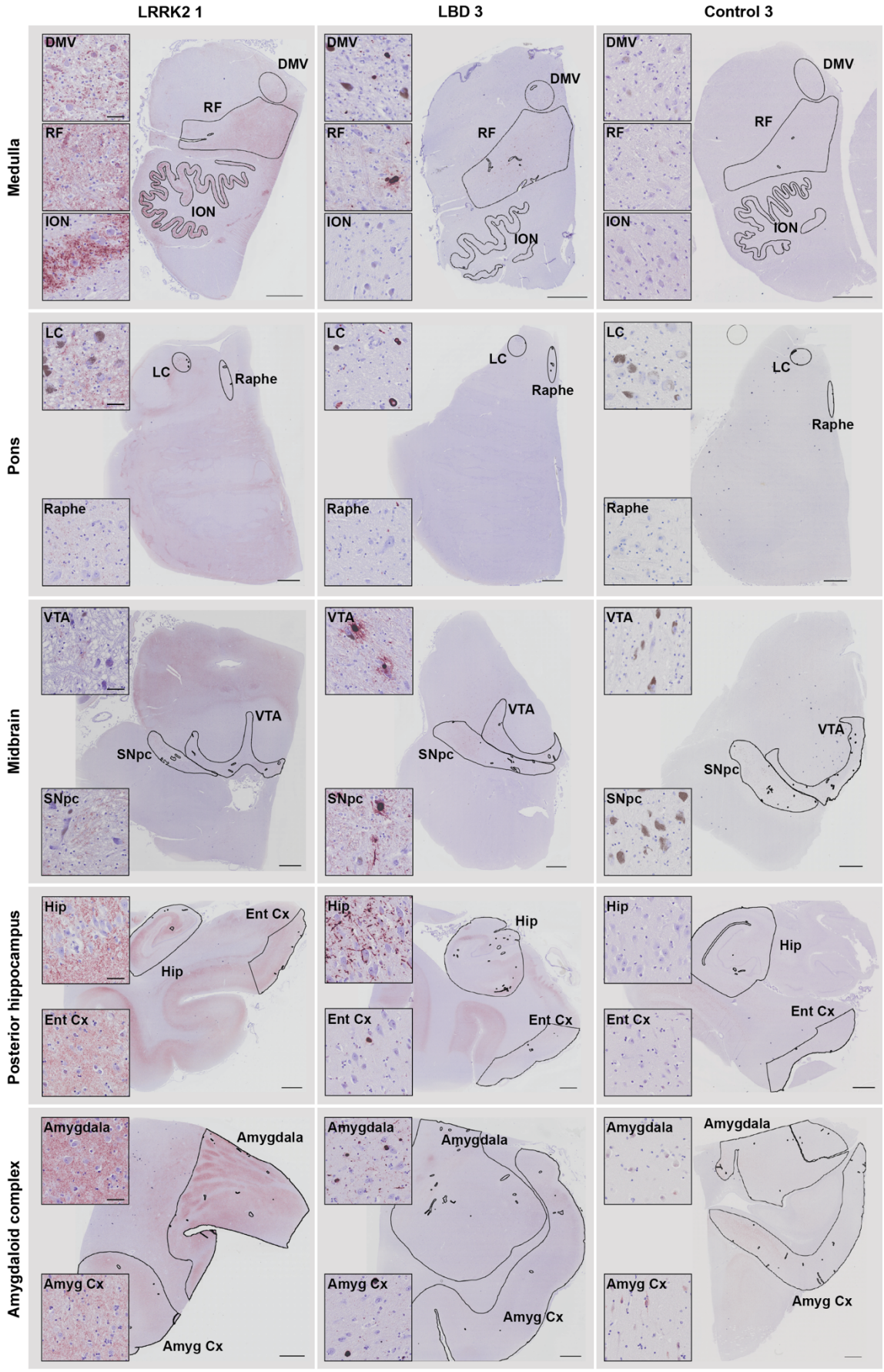

Suppl. Fig. 1 Delineation of regions of interest for quantitative PLA analyses

Full slide scans and magnified panels from three different cases and all five regions (medulla, pons, midbrain, posterior hippocampus, and amygdaloid complex) stained for each case. Regions of interest for quantitative analysis are outlined in black in each tissue section, while magnified panels show representative staining in the indicated regions. DMV = dorsal motor nucleus of the vagus, RF = reticular formation, ION = inferior olivary nucleus, LC = locus coeruleus, Raphe = raphe nucleus, SNpc = substantia nigra pars compacta, VTA = ventral tegmental area, Hip = hippocampus, Ent Cx = entorhinal cortex, Amyg Cx = Amygdaloid cortex. Scale bars = 2 mm (overview images), 50 µm (insets, applies to all images).

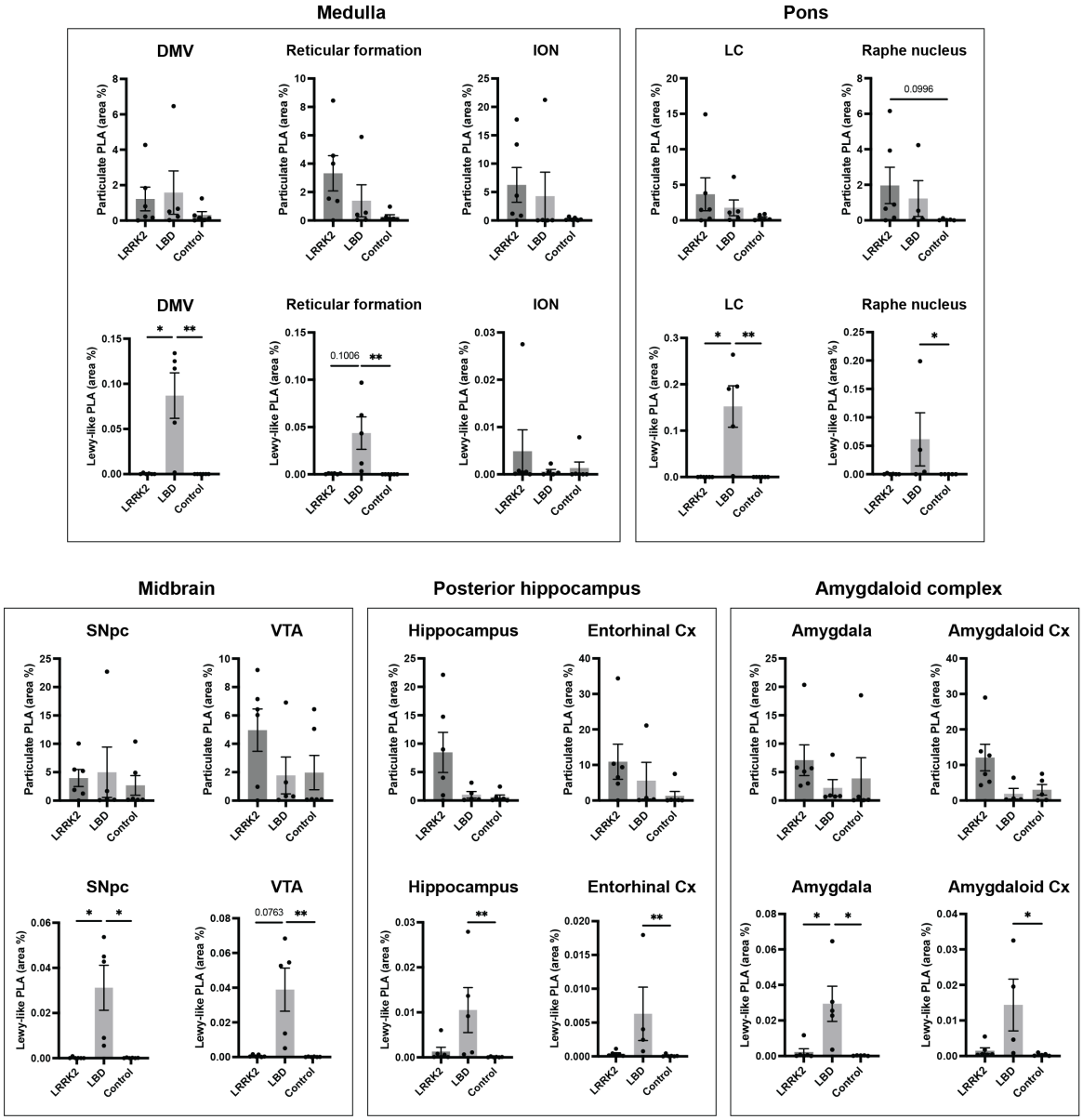

Suppl. Fig. 2 Particulate PLA and Lewy-like PLA area coverage in various subregions

Particulate PLA coverage (top) and Lewy-like PLA coverage (bottom) in subregions of the medulla, pons, midbrain, posterior hippocampus, and amygdaloid complex. All graphs show mean ± SEM with data points for individual cases. Analysed with Kruskal-Wallis one-way ANOVA followed by Dunn's multiple comparison test. * $p<0.05$, ** $p<0.01$, *** $p<0.001$.

Suppl. Table 1 Fold difference in area coverage of signal between particulate PLA and Lewy-like PLA for LBD cases

	LBD 1	LBD 2	LBD 3	LBD 4	LBD 5	Average
Medulla	121.09	10.85	12.40	56.59	7.26	41.64
Pons	39.76	51.87	14.09	184.51	12.89	60.62
Midbrain	272.23	34.23	24.36	18.87	5.64	71.07
Posterior hippocampus	983.56	242.41	286.16	115.90	41.10	333.83
Amygdaloid complex	174.80	239.65	28.66	46.65	14.84	100.92

Suppl. Table 2 Reported neuropathological findings in LRRK2 mutation carriers.

Study Centre	No. cases	Mutation and clinical diagnosis[a]	αSyn antibody	Pathological findings	
				LB pathology	Non-LB pathology
Henderson et al. 2019 [28] Center for Neuro-degenerative Disease Research, UPenn, US	11	9 with G2019S mutation (7 with PD, 2 with PDD) 1 with L1165P (PDD) 1 with R793M (PDD)	pSer129	**64% (7/11)** prominent αSyn pathology (substantia nigra, amygdala, hippocampus and cingulate cortex but no staging given)	**36% (4/11)** variable AD-like tau pathology
Blauwendraat et al. 2019 [6] Johns Hopkins Brain Resource Center, US	6	G2019S mutation (2 with PD, 3 with PDD, 1 with parkinsonism)	N/A	**33% (2/6)** 1 with neocortical LBD (+AD pathology) 1 with limbic LBD (+AD pathology)	**67% (4/6)** 3 with tau pathology (PSP-like) 1 with unspecific nigral cell loss
Sanchez-Contreras et al. 2017 [54] Mayo Clinic Florida brain bank, US	4	1 with G2019S (probable PSP) 1 with R1441C (probable PSP) 1 with A1413T (PSP) 1 with R1707K (AD-type dementia)	N/A	- (screened cohort only consisted of PSP and CBD)	**100% (4/4)** 2 pure PSP 1 PSP (+AD pathology) 1 CBD (+AD pathology)
Ling et al. 2013 [36] Queen Square Brain Bank, UCL, UK	1	G2019S mutation and Q124E in MAPT (PD)	pSer129, KM51	-	**100% (1/1)** AD-type tau pathology (Braak tau stage III, CERAD B, Thal phase 3) and sparse TDP-43 pathology
Poulopoulos et al. 2012 [48] Columbia University Brain bank, New York, US	3	G2019S mutation (1 PD, 2 PDD)	N/A	**100% (3/3)** 1 with neocortical LBD (+AD pathology) 1 with neocortical LBD 1 brainstem LBD	-
Ujiie et al. 2012[b] [65] Department of Pathology, Kanagawa, Japan	6[b]	I2020T mutation (all with PD)	pSer129	**17% (1/6)** 1 with LB pathology (distribution not reported)	**83% (5/6)** 2 with mild AD-type pathology (Braak stage 2 and 3) 2 with brainstem NFTs alone 1 with unspecific nigral loss
Puschmann et al. 2012 [49] Lund University, Sweden	1	N1437H mutation (PD)	LB509	**100% (1/1)** neocortical LBD with prominent ubiquitin pathology, also in white matter	-
Ruffmann et al. 2012 [53] Division of Pathology, Milan, Italy	1	G2019S mutation (PDD)	4D6	-	**100% (1/1)** 1 with tau pathology (PSP-like)

Gomez and Ferrer 2010 [23] Hospital Bellvitge, University of Barcelona, Spain	3	G2019S mutation (PD)	pSer129, Chemicon, Syn 505	**67% (2/3)** 2 limbic DLB	**33% (1/3)** Unspecific nigral cell loss
Martí-Massó et al. 2009 [40] Pathologic Anatomy Department, San Sebastian, Spain	1	R1441G mutation (PD)	pSer129, Novocastra, Chemicon, Syn 505	-	**100% (1/1)** Unspecific nigral cell loss
Covy et al. 2009 [11] Department of Pathology, UPenn, US	2	1 with R793M mutation (PD) 1 with L1165P mutation (PDD)	pSer129, LB509, Syn 514, Syn 21, In-house SNL4 against aa 2-12	**100% (2/2)** Neocortical DLB with occasional TDP-43 pathology in temporal cortex	-
Hasegawa et al. 2009[b] [27] Sagamihara National Hospital, Japan	8[b]	I2020T mutation (PD)	pSer129	**12% (1/8)** 1 with brainstem LBD	**88% (7/8)** 6 with unspecific nigral cell loss 1 with MSA-P type pathology
Giordana et al. 2007 [22] Department of Neuroscience, University of Torino, Italy	1	I1371V mutation (PD)	KM51, LB509, Syn1	**100% (1/1)** Limbic LBD (+AD pathology)	-
Gaig et al. 2007 [18] Hospital Clinic, University of Barcelona, Spain	1	G2019S mutation (PD)	N/A	-	**100% (1/1)** Unspecific nigral cell loss
Dächsel et al. 2007 [12] Mayo Clinic Florida brain bank, US	1	G2019S mutation (no detailed clinical data but dementia and tremor)	N/A	-	**100% (1/1)** Ubiquitin-IR inclusion alone, similar to FTLD-U
Giasson et al. 2006 [20] Department of Pathology, UPenn, US	3	G2019S mutation (parkinsonism)	LB509, Syn 505	**67% (2/3)** 1 with neocortical LBD (+AD pathology) 1 with brainstem LBD	**33% (1/3)** 1 with unspecific nigral cell loss

Ross et al. 2006 [52] Mayo Clinic Florida brain bank, US	8	G2019S mutation (PD)	N/A	**100% (8/8)** 4 with brainstem LBD 3 with limbic LBD 1 with neocortical LBD	-
Rajput et al. 2006 [50] Royal University Hospital, Saskatoon, Canada	3	G2019S mutation (PD)	LB509	-	**100% (3/3)** 2 with tau pathology (PSP-like) 1 with argyrophilic grain disease
Khan et al. 2005 [34] Queen square Brain Bank, UCL, UK	1	Y1699C mutation (PD)	N/A	**100% (1/1)** Brainstem LBD	-
Gilks et al. 2005 [21] Queen square Brain Bank, UCL, UK	3	G2019S mutation (PD)	N/A	**100% (3/3)** 1 with brainstem LBD 2 with limbic LBD	-
Wszolek et al. 2004[c] [69] Mayo Clinic Florida brain bank, US	4[c]	R14441C mutation (3 with PD and 1 with PSP)	N/A	**50% (2/4)** 1 with brainstem LBD 1 with neocortical LBD	**50% (2/4)** 1 with PSP-like tau pathology 1 with unspecific nigral cell loss
Zimrich et al. 2004[c] [72] Mayo Clinic Florida brain bank, US	4[c]	R14441C mutation (3 with PD and 1 with PSP)	N/A	**50% (2/4)** 1 with brainstem LBD 1 with neocortical LBD	**50% (2/4)** 1 with PSP-like tau pathology 1 with unspecific nigral cell loss
Wszolek et al. 1997 [70] University of Nebraska Medical Center, Omaha, US	2	Y1699C mutation (PD)	None (Ubiq-uitin)	-	**50% (1/2)** Both cases had nigral cell loss without LB pathology (one with AD pathology)
TOTAL	**68**			**33 (48.5%)**	**35 (51.5%)**

Abbreviations: AD = Alzheimer's disease, CBD = corticobasal degeneration, FTLD-U = frontotemporal lobar degeneration with ubiquitin-positive inclusions, LBD = Lewy body disease, MSA-P = multiple system atrophy parkinsonism-subtype, NFTs = neurofibrillary tangles, PSP = progressive supranuclear palsy.
[a] Unless otherwise stated, mutations listed all pertain to LRRK2. Where available, clinical diagnosis is listed in brackets.
[b] These two studies have same cases.
[c] These two studies have same cases.